

SCIENTIFIC REPORTS



OPEN

Design, synthesis and structure-activity relationship of 3,6-diaryl-7*H*-[1,2,4]triazolo[3,4-*b*][1,3,4]thiadiazines as novel tubulin inhibitors

Qile Xu¹, Kai Bao¹, Maolin Sun¹, Jingwen Xu², Yueting Wang¹, Haiqiu Tian¹, Daiying Zuo², Qi Guan¹, Yingliang Wu² & Weige Zhang¹

A novel series of 3,6-diaryl-7*H*-[1,2,4]triazolo[3,4-*b*][1,3,4]thiadiazines were designed, synthesized and biologically evaluated as vinylogous CA-4 analogues, which involved a rigid [1,2,4]triazolo[3,4-*b*][1,3,4]thiadiazine scaffold to fix the configuration of (*Z,E*)-butadiene linker of A-ring and B-ring. Among these rigidly vinylogous CA-4 analogues, compounds 4d, 5b, 5i, 6c, 6e, 6g, 6i and 6k showed excellent antiproliferative activities against SGC-7901, A549 and HT-1080 cell lines with IC₅₀ values at the nanomolar level. Compound 6i showed the most highly active antiproliferative activity against the three human cancer cell lines with an IC₅₀ values of 0.011–0.015 μM, which are comparable to those of CA-4 (IC₅₀ = 0.009–0.013 μM). Interestingly, SAR studies revealed that 3,4-methylenedioxyphenyl, 3,4-dimethoxyphenyl, 3-methoxyphenyl and 4-methoxyphenyl could replace the classic 3,4,5-trimethoxyphenyl in CA-4 structure and keep antiproliferative activity in this series of designed compounds. Tubulin polymerization experiments showed that 6i could effectively inhibit tubulin polymerization, which was corresponded with CA-4, and immunostaining experiments suggested that 6i significantly disrupted microtubule/tubulin dynamics. Furthermore, 6i potently induced cell cycle arrest at G₂/M phase in SGC-7901 cells. Competitive binding assays and docking studies suggested that compound 6i binds to the tubulin perfectly at the colchicine binding site. Taken together, these results revealed that 6i may become a promising lead compound for new anticancer drugs discovery.

Microtubules are composed of dynamic polymers of α- and β-tubulin subunits, which play an essential role in a variety of fundamental cell functions including the maintenance of cell shape, intracellular transport and cell division^{1,2}. Due to the multiple functions of microtubules in cell mitosis, tubulin has become a highly attractive target for new anticancer drugs discovery^{3,4}. Microtubule-targeting drugs normally can be grouped into microtubule stabilizing and microtubule destabilizing drugs that disrupt tubulin/microtubule dynamics by binding to the protein tubulin leading to cell death^{5,6}. Microtubule-targeting drugs are known to interact with tubulin through many binding sites: the laulimalide, taxane/epothilone, taccolonolide, vinca alkaloid and colchicine sites. Paclitaxel, colchicine, and vinblastine represent the well-known three major types of tubulin binding agents which bind at three major sites on tubulin: the taxane, colchicine, and vinca alkaloid sites, respectively^{7,8}. While clinically applied microtubule targeting drugs binding at the vinca alkaloid or taxanes sites in tubulin are greatly successful, there are no clinically applied colchicine-binding site anticancer drugs currently available⁹.

Combretastatin A-4 (CA-4, 1, Fig. 1) is one of the most antiproliferative agents that bind at the colchicine binding site of tubulin¹⁰. Structure-activity relationship studies for CA-4 have shown that the *cis*-olefin bond (*Z*-alkene) and the presence of a 3,4,5-trimethoxyphenyl were essential for the activity¹¹. Unfortunately, the

¹Key Laboratory of Structure-Based Drug Design and Discovery, Ministry of Education, Shenyang Pharmaceutical University, 103 Wenhua Road, Shenhe District, Shenyang, 110016, China. ²Department of Pharmacology, Shenyang Pharmaceutical University, 103 Wenhua Road, Shenhe District, Shenyang, 110016, China. Qile Xu and Kai Bao contributed equally to this work. Correspondence and requests for materials should be addressed to Y.W. (email: yingshuang_1016@163.com) or W.Z. (email: zhangweige@syphu.edu.cn)

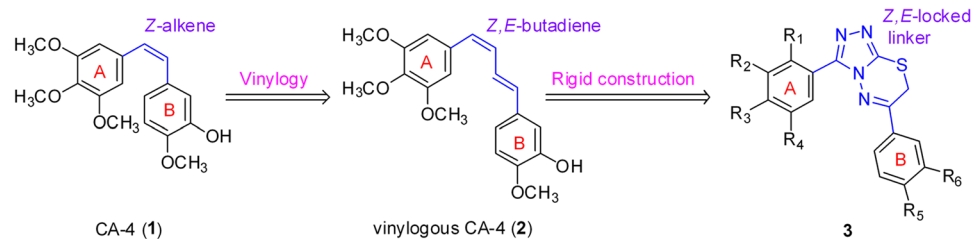


Figure 1. Structures of known tubulin inhibitors and design strategy for the target compounds.

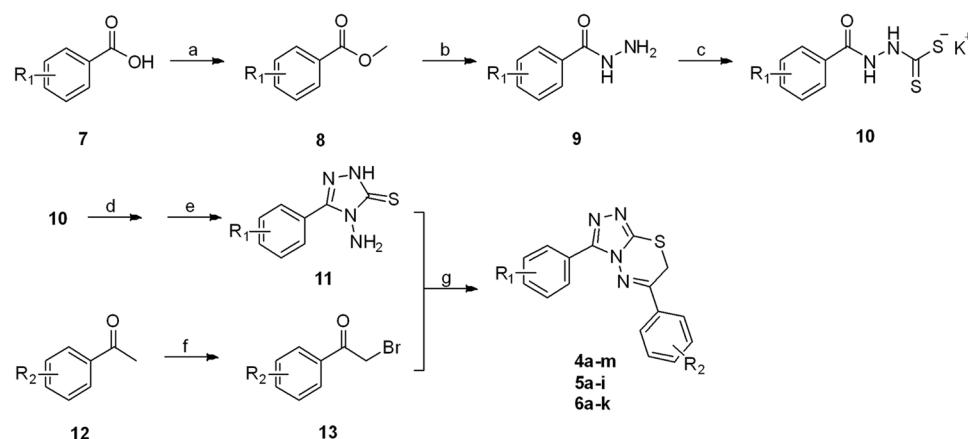


Figure 2. Reagents and conditions: (a) MeOH, conc. H_2SO_4 , MW, 70°C .; (b) $\text{N}_2\text{H}_4\cdot\text{H}_2\text{O}$, MeOH, reflux; (c) CS_2 , KOH, MeOH, 25°C .; (d) $\text{N}_2\text{H}_4\cdot\text{H}_2\text{O}$, H_2O , MW, 100°C .; (e) HCl, 0°C .; (f) CuBr_2 , CHCl_3 , EtOAc, reflux; (g) EtOH, MW, 80°C .

Z-alkene of CA-4 tends to isomerize to the more stable but inactive E-alkene under the external conditions of light, heat, and protic media, resulting in a dramatic reduction in both antitubulin and antiproliferative activities^{9,12}.

In the past several years, a wide variety of CA-4 analogues have been reported^{13–25}. The modifications of CA-4 analogues can be generally classified into three major classes²³: (I) introducing an extended side chain to the B ring; (II) replacing the alkene linker with another flexible linker such as a carbonyl, a methylene, or another suitable connection group; (III) replacing the alkene linker with a conformational rigid heterocyclic linker.

Accordingly, replacement of the *cis*-olefin bond by rigid heterocycle rings (such as five-membered and six-membered rings) that facilitate a Z-restricted configuration has proven to be one of the most effectively strategies in maintaining both antiproliferative and antitubulin activity^{26–29}. The vinylogous CA-4 (2, Fig. 1) with a (Z,E)-butadiene linker has potent antiproliferative and tubulin polymerization inhibitory activity, but the main problem is that it tends to isomerize to the more stable but inactive (E,E)-isomeric derivative³⁰. To the best of our knowledge, no report has attempted to lock the Z,E-configuration of vinylogous CA-4 with a rigid fused heterocycle to maintain biological activities.

The unique [1,2,4]triazolo[3,4-b][1,3,4]thiadiazine scaffold which was fused by triazole and thiadiazine represents an important kind of nitrogen heterocyclic with a broad spectrum of biological activities including anticancer activity^{31,32}. As one of our research directions^{33–37}, here we designed a series of 3,6-diaryl-7H-[1,2,4]triazolo[3,4-b][1,3,4]thiadiazines as vinylogous CA-4 analogues with general structure 3, in which the (Z,E)-butadiene linker of vinylogous CA-4 was replaced with a novel rigid [1,2,4]triazolo[3,4-b][1,3,4]thiadiazine scaffold (Fig. 1). To explore the SAR of vinylogous CA-4 analogues, various substituents were introduced at different positions of the B-ring. Specifically we also have attempted to make modifications on the classical trimethoxy A-ring, although the 3,4,5-trimethoxyphenyl is a crucial fragment in CA-4, vinylogous CA-4 and their analogues³⁸. Thirty three target compounds were synthesized and classified into the following three groups according to the A-ring substituents: (I) 2,3,4-trimethoxyphenyl (4a–m), (II) 3,4,5-trimethoxyphenyl (5a–i), (III) other A-ring substituent (6a–k). The representative compound 61 was selected to investigate its mechanism of action. Besides, molecular modeling studies with the colchicine binding site of tubulin were performed with the most potent compound 61.

Result and Discussion

Chemistry. The target compounds 4a–m, 5a–i and 6a–k were prepared as outlined in Fig. 2. The substituted benzoic acids 7 were reacted with excess methanol with concentrated sulfuric acid as catalyst to afford the corresponding esters 8 which were further reacted with 80% hydrazine monohydrate in methanol to get hydrazides

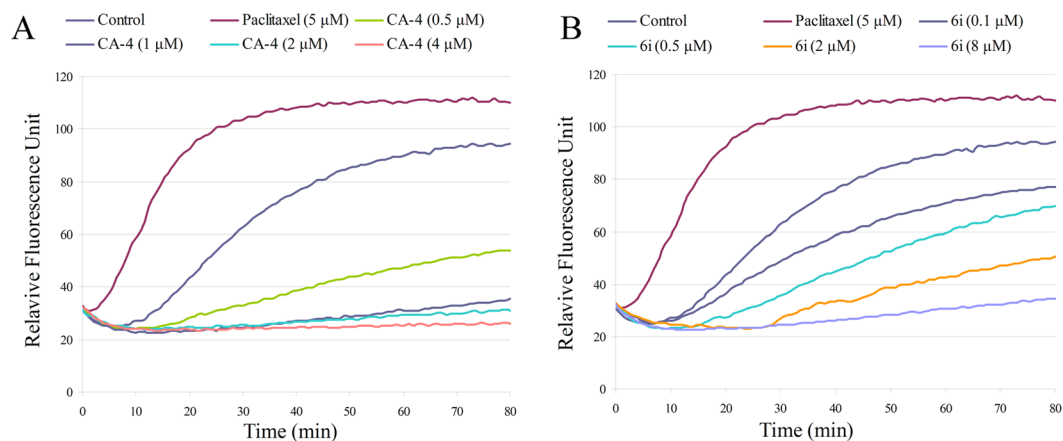


Figure 3. (A) CA-4 inhibits microtubule polymerization *in vitro*. (B) Compound **6i** inhibits microtubule polymerization *in vitro*. Tubulin was mixed with reaction buffer and incubated with CA-4 (0.5, 1, 2, 4 μM), paclitaxel (5.0 μM), **6i** (0.1, 0.5, 2.0, 8.0 μM) or vehicle DMSO (control). The reaction was monitored at 37 °C.

9 under microwave (250 W, 70 °C) irradiation. The hydrazides **9** were reacted with carbon disulphide and potassium hydroxide in methanol to give corresponding dithiocarbazines **10** and then dithiocarbazines **10** further reacted with excess 80% hydrazine monohydrate to get the key intermediate aryl triazoles **11**. On the other hand, the commercially available starting acetophenones **12** were subjected to α -bromination with copper bromide in refluxing chloroform/ethyl acetate to get α -bromoacetophenones **13**. Finally, α -bromoacetophenones **13** were reacted with aryl triazoles **11** to afford the target compounds in ethanol within 5 min under microwave (250 W, 80 °C) irradiation in the absence of catalysts.

In vitro anti-proliferative activity. *In vitro* antiproliferative activity against three human cancer cell lines, including gastric adenocarcinoma SGC-7901 cells, lung adenocarcinoma A549 cells and fibrosarcoma HT-1080 cells, was determined using a standard MTT assay with CA-4 as the positive control. As shown in Table 1, it is evident that most of these new compounds showed moderate to excellent antiproliferative activity, indicating that the utilization of the rigid [1,2,4]triazolo[3,4-b][1,3,4]thiadiazine scaffold to lock the (*Z,E*)-butadiene linker of vinylogous CA-4 is an effective strategy to maintain potent antiproliferative activity. When A-ring was a 2,3,4-trimethoxyphenyl, compounds **4a–m** displayed only modest antiproliferative activity. Interestingly, the 4-methyl-substituted (B-ring) compound **4d** displayed the most active antiproliferative activity (0.028–0.073 μM); however, compound **4j** (B-ring was a 3-amino-4-methoxyphenyl) and **4l** (B-ring was a 3-hydroxy-4-methoxyphenyl) exhibited only moderate activity. Compared to the 2,3,4-trimethoxyphenyl-substituted **4a–m**, 3,4,5-trimethoxy substitution at A-ring tended to enhance the potency of corresponding compounds **5a–i**. Among compounds **5a–i**, 4-methyl-substituted (B-ring) **5b** displayed the most potent antiproliferative activity with IC_{50} values of 0.016–0.027 μM and compound **5i** also effectively inhibited the three cell lines growth with IC_{50} values of 0.026–0.071 μM.

We further examined the cytotoxic effect of **6a–k** by replacement of trimethoxy substituents with other substituents (3,4-methylenedioxy, 3,4-dimethoxy, 3-methoxy, 4-methoxy) at A-ring along with various substituents at ring B. Surprisingly, compounds **6c**, **6e**, **6g**, **6i** and **6k** displayed nanomolar IC_{50} values against all tested cells and compound **6i** with a 3-methoxyphenyl at A-ring showed the most potent antiproliferative activity with an IC_{50} of 0.011–0.015 μM (comparable to CA-4 with an IC_{50} of 0.009–0.013 μM). These results clearly indicated that the classic 3,4,5-trimethoxyphenyl in CA-4 structure could be replaced by 3,4-methylenedioxyphenyl, 3,4-dimethoxyphenyl, 3-methoxyphenyl and 4-methoxyphenyl without significant reduction of antiproliferative activity in this series of designed compounds. A comparison of vinylogous CA-4 (*Z,E*) with the current compound **6i** (Table S1) was included in the Supporting Information.

Tubulin assembly. To investigate whether the antiproliferative activity was produced by interaction between the target compounds and tubulin, the most active compound **6i** was investigated for its inhibition of tubulin polymerisation. This assay uses highly purified tubulin from porcine brain. CA-4 (**1**) and paclitaxel were used as positive and negative controls, respectively (Fig. 3A). As shown in Figs 3B, **6i** effectively inhibited tubulin polymerization with an IC_{50} value of 1.6 μM, which was slightly higher to that of CA-4 (IC_{50} = 0.92 μM). The representative raw data for the polymerization assay of compound **6i** and CA-4 showed that both of them caused a dose-dependent inhibition of tubulin polymerization; in contrast, paclitaxel, a microtubule stabilizing agent, could distinctly promoted this process (Fig. 3). Thus, the results indicated that **6i** was a tubulin inhibitor.

Immunofluorescence studies. To directly test **6i** can target microtubule/tubulin, we treated SGC-7901 cells with 2-fold IC_{50} of **6i** and analyzed microtubules by immunocytochemistry staining. CA-4 was employed as positive control in this experiment. As illustrated in Fig. 4, the control cells displayed well-organized microtubule network throughout the cells. After treatment with **6i** and CA-4 (at their respective 2-fold IC_{50} concentrations,

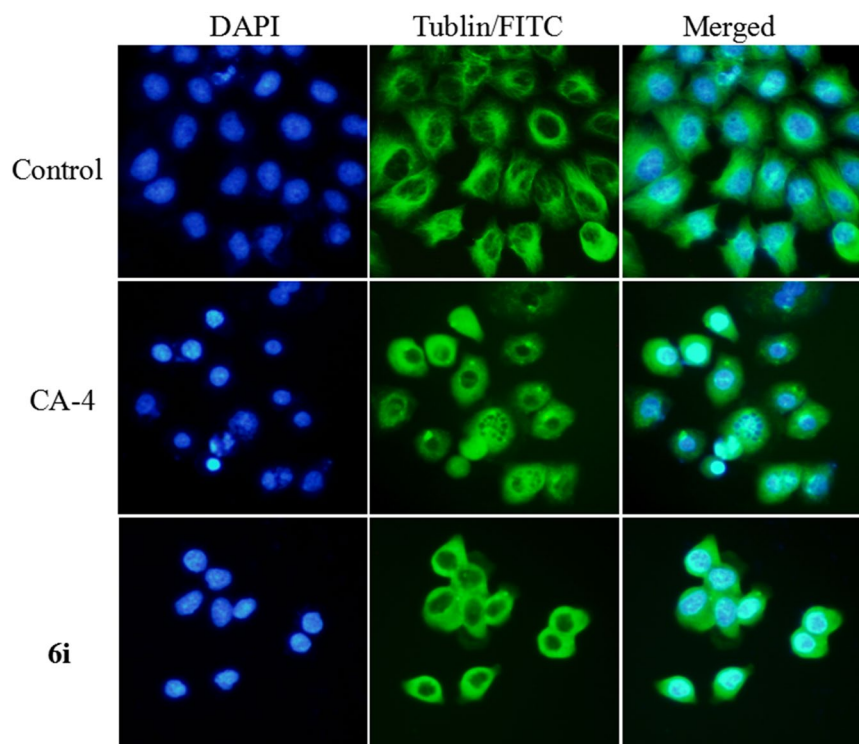


Figure 4. Effects of **6i** on tubulin network of SGC-7901 cells by immunofluorescence. SGC-7901 cells were treated with DMSO (vehicle control), CA-4 (0.022 μM) or **6i** (0.022 μM) for 12 h. The left and middle panels represent the tubulin assembly stained with DAPI and FITC and the right panel represents a merge of the corresponding left and middle panels.

respectively), microtubules became irregular arrangement and organization, and the tubulin network showed a disruption. These results further confirmed that the target of **6i** was tubulin.

Cell cycle analysis. It is well known that tubulin inhibitors such as colchicine and CA-4 arrest cell cycle distribution in G_2/M phase. Thus, the effect of compound **6i** on the cell cycle progression of the SGC-7901 cells was investigated by flow cytometry analysis (Fig. 5). The SGC-7901 cells were treated with compound **6i** (1-, 2-, 4-fold IC_{50}) for 12 h, and CA-4 (2-fold IC_{50}) was used as a positive control. Flow cytometry analysis showed that both **6i** and CA-4 caused a potent cell cycle arrests in G_2/M phase. In comparison, the untreated cells (control) showed normal distribution with more cell population in the G_1 phase. Compound **6i** could arrest cell cycle distribution at the G_2/M phase in a dose-dependent manner. Moreover, compound **6i** was found to cause subsequent apoptosis after G_2/M arrest in SGC-7901 cells (Figure S1).

Competitive tubulin-binding assay. To confirm whether these designed compounds could bind to the colchicine site on tubulin, compound **6i** was investigated for its ability of competitive inhibition of colchicine binding^{39,40}. CA-4 and paclitaxel were used as a positive and a negative control, respectively. The intrinsic fluorescence of colchicine increases upon binding to the tubulin, which could be used as an index for **6i** or CA-4 competition with colchicine in tubulin binding. As shown in Fig. 6, the fluorescence of a colchicine-tubulin complex was reduced in the presence of CA-4 or **6i** in a dose-dependent manner. These observations indicated that they inhibit the binding of colchicine to the tubulin, thereby suggesting the direct binding of compound **6i** at the colchicine binding site of tubulin.

Molecular docking studies. Molecular docking studies were performed by using the CDocker program in Discovery Studio 3.0 software to explore the binding ability of **6i** to the colchicine binding site of tubulin (PDB: 1SA0). Docking studies revealed that the compound **6i** coincides closely with CA-4 and vinylogous CA-4, and they occupied the colchicine binding site of α,β -tubulin mostly buried in the β subunit (Fig. 7A). For compound **6i**, a hydrogen bond formed between the oxygen atom of methoxyl group and the thiol group of Cys β 241 (note: in some publications this residue is numbered as Cys β 239)⁹. The nitrogen atom of the amino group on the B-ring formed another hydrogen bond with the residue of Asn β 349. Additionally, the nitrogen atom on triazolothiadiazine linker of compound **6i** formed a direct hydrogen bond with the residue of Ala β 250 (Fig. 7B). The results of docking studies suggested that compound **6i** binds to the tubulin possibly at the colchicine binding site on tubulin, albeit with lesser affinity than CA-4.

In summary, we designed and synthesized a novel series of 3,6-diaryl-7H-[1,2,4]triazolo[3,4-b][1,3,4]thiadiazines as analogues of vinylogous CA-4. Among them, compounds **4d**, **5b**, **5i**, **6c**, **6e**, **6g**, **6i** and **6k** showed

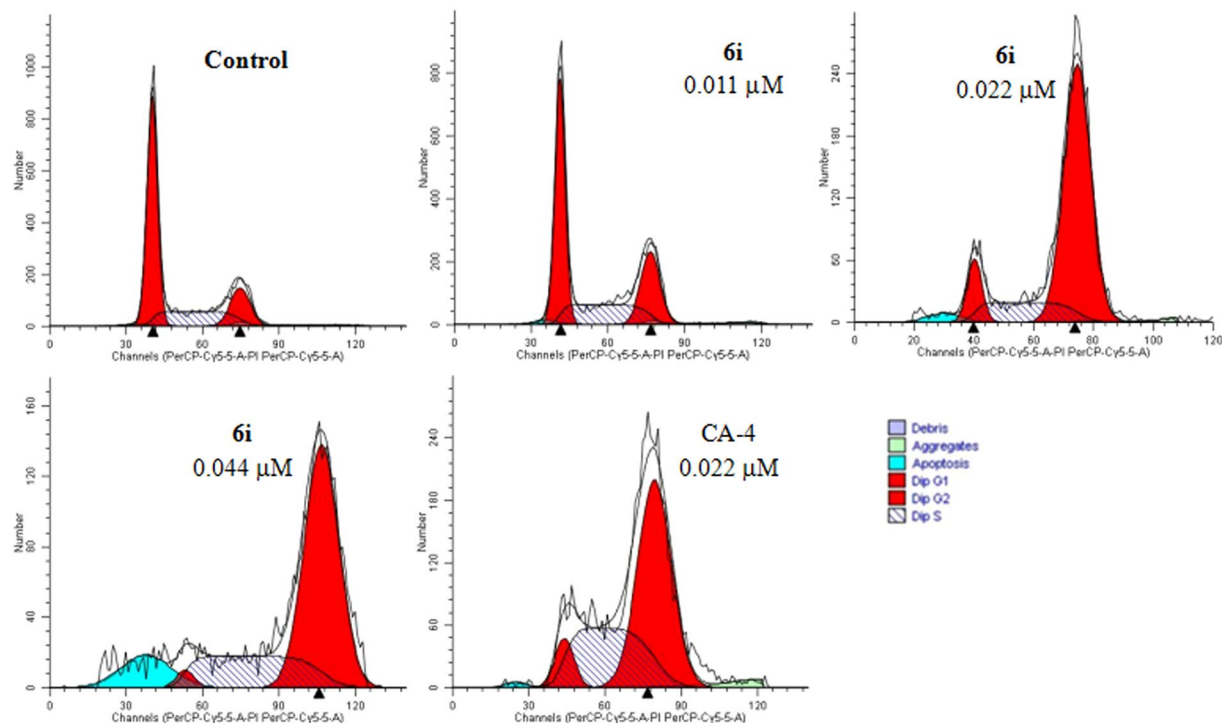


Figure 5. Compound **6i** affects the cell cycle progression in SGC-7901 cells. SGC-7901 cells were treated with compound **6i** (0.011, 0.022 and 0.044 μM , respectively) or CA-4 (0.022 μM) for 12 h.

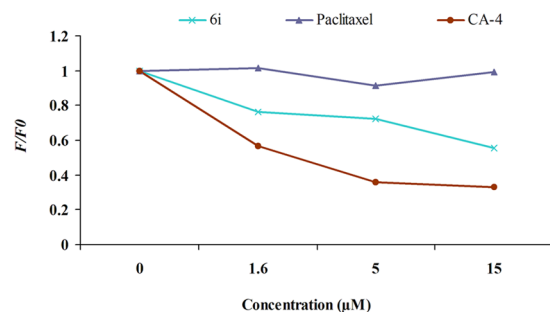


Figure 6. Competitive binding of **6i** to colchicine-binding site on tubulin. F/F_0 represents inhibition rate ($IR = F/F_0$) whereas F_0 refers to fluorescence of the 5.0 μM colchicine-tubulin complex, and F describes the fluorescence of a given concentration (1.6 μM , 5.0 μM , and 15.0 μM) of CA-4, compounds **6i** and paclitaxel competition with the 5.0 μM colchicine-tubulin complex.

excellent antiproliferative activities against SGC-7901, A549 and HT-1080 cell lines with IC_{50} values at nanomolar level. Compound **6i** with a 3-methoxyphenyl in place of the classic trimethoxyphenyl A-ring, showed the most potent antiproliferative activity with an IC_{50} of 0.011–0.015 μM , which was comparable to that of CA-4 (0.009–0.013 μM). The tubulin polymerization and immunofluorescence experiments showed that **6i** effectively inhibited tubulin polymerization and resulted in a disruption on the tubulin network in SGC-7901 cells. Furthermore, **6i** caused a potent cell cycle arrest in G_2/M phase in a dose-dependent manner. Competitive binding assay and molecular docking studies indicated that compound **6i** binds to the colchicine binding site of tubulin.

Taken together, a novel rigid [1,2,4]triazolo[3,4-b][1,3,4]thiadiazine scaffold was applied to lock the (*Z,E*)-butadiene linker of A-ring and B-ring of vinylogous CA-4 and proved to be a successful strategy in retaining both antiproliferative and antitubulin activities. For the new skeleton, it is worth noting that 3,4-methylenedioxyphenyl, 3,4-dimethoxyphenyl, 3-methoxyphenyl and 4-methoxyphenyl could replace the crucially classic 3,4,5-trimethoxyphenyl in CA-4 and vinylogous CA-4. The present study not only resulted in a series of excellent tubulin inhibitors, but transcended the common understanding of structure-activities relationships of CA-4, vinylogous CA-4 and their analogues. Further modifications of these novel CBSIs and detailed mechanistic studies for the anticancer properties are underway in our lab.

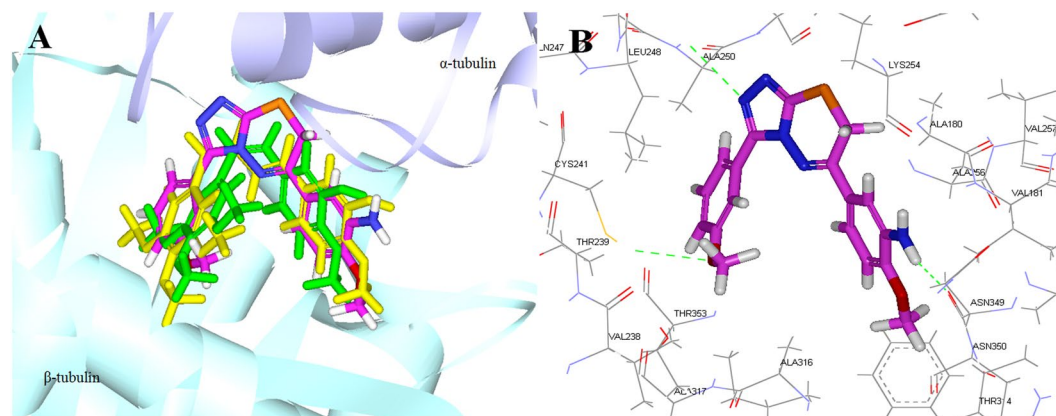


Figure 7. (A) Overlay of **6i** (pink), CA-4 (green) and vinylogous CA-4 (yellow) in the colchicine binding site. (B) The hydrogen bond interactions are displayed as green dotted lines and the amino acids are displayed as stick models.

Methods

Reagents and equipment. All solvents and chemical reagent were got from commercially available sources and were used without purification. The microwave reactions were performed on a discover-sp single mode microwave reactor from CEM Corporation. The progress of reactions was monitored by TLC using silica gel plates under UV light. NMR spectra were recorded on a Bruker AVANCE 400, or 600 spectrometer (^1H , 400 MHz, 600 MHz; ^{13}C , 100 MHz, 150 MHz), in CDCl_3 or $\text{DMSO}-d_6$ (TMS as internal standard). Chemical shifts are expressed as parts per million downfield from tetramethylsilane. Mass spectra (MS) were measured on an Agilent 1100-sl mass spectrometer with an electrospray ionisation source. Melting points were measured on a hot stage microscope (X-4, Beijing Taikete Ltd.) and are uncorrected.

General synthetic procedures for target compounds. To a solution of appropriately intermediates **11** (10 mmol) in absolute ethyl alcohol (15 mL), was added the appropriate α -bromoacetophenones **13** (10 mmol). The mixture was heated under microwave irradiation at 80°C for 30 min. After the reaction completed, water was then added to the mixture and the precipitate formed was collected and crystallized from the proper solvent. Reduction of the nitro groups of **4i**, **5f**, **6b**, **6f**, **6h** and **6j** in a mixture of hydrazine hydrate, ferric chloride hexahydrate and activated carbon in methanol provided the corresponding **4j**, **5g**, **6c**, **6g**, **6i** and **6k**, respectively³³. Debonylation of compounds **4k**, **5h** and **6d** with titanium tetrachloride afforded, respectively the phenol derivatives, **4l**, **5i** and **6e**³³.

3-(2,3,4-Trimethoxyphenyl)-6-(4-fluorophenyl)-7H-[1,2,4]triazolo[3,4-b][1,3,4]thiadiazine (4a). White solid; yield: 65%; M.p.: $92\text{--}94^\circ\text{C}$; $^1\text{H-NMR}$ (400 MHz, CDCl_3): δ 7.81–7.85 (m, 2 H), 7.32 (d, $J=8.6$ Hz, 1 H), 7.11–7.15 (m, 2 H), 6.78 (d, $J=8.6$ Hz, 1 H), 3.98 (s, 2 H), 3.93 (s, 3 H), 3.87 (s, 3 H), 3.77 (s, 3 H); $^{13}\text{C-NMR}$ (100 MHz, CDCl_3): δ 166.1, 163.6, 156.0, 152.7, 151.8, 142.0, 141.1, 129.7, 126.5 (d, $J=8.8$ Hz, 2 C), 126.2, 116.2 (d, $J=21.8$ Hz, 2 C), 112.9, 107.1, 61.6, 60.9, 56.1, 23.5; ESI-MS: $m/z=401.3$ $[\text{M}+\text{H}]^+$, 423.2 $[\text{M}+\text{Na}]^+$.

3-(2,3,4-Trimethoxyphenyl)-6-(4-chlorophenyl)-7H-[1,2,4]triazolo[3,4-b][1,3,4]thiadiazine (4b). White solid; yield: 82%; M.p.: $88\text{--}90^\circ\text{C}$; $^1\text{H-NMR}$ (400 MHz, CDCl_3): δ 7.75 (d, $J=8.6$ Hz, 2 H), 7.39 (d, $J=8.6$ Hz, 2 H), 7.29 (d, $J=8.7$ Hz, 1 H), 6.77 (d, $J=8.7$ Hz, 1 H), 3.98 (s, 2 H), 3.92 (s, 3 H), 3.86 (s, 3 H), 3.74 (s, 3 H); $^{13}\text{C-NMR}$ (100 MHz, CDCl_3): δ 155.9, 152.6, 151.7, 151.7, 141.9, 141.0, 138.0, 131.9, 129.2 (2 C), 128.5 (2 C), 126.1, 112.8, 107.0, 61.5, 60.8, 56.0, 23.3; ESI-MS: $m/z=417.3$ $[\text{M}+\text{H}]^+$, 439.2 $[\text{M}+\text{Na}]^+$.

3-(2,3,4-Trimethoxyphenyl)-6-(4-bromophenyl)-7H-[1,2,4]triazolo[3,4-b][1,3,4]thiadiazines (4c). White solid; yield: 63%; M.p.: $96\text{--}98^\circ\text{C}$; $^1\text{H-NMR}$ (400 MHz, CDCl_3): δ 7.68 (d, $J=8.6$ Hz, 2 H), 7.56 (d, $J=8.6$ Hz, 2 H), 7.30 (d, $J=8.7$ Hz, 1 H), 6.78 (d, $J=8.7$ Hz, 1 H), 3.98 (s, 2 H), 3.92 (s, 3 H), 3.86 (s, 3 H), 3.75 (s, 3 H); $^{13}\text{C-NMR}$ (100 MHz, CDCl_3): δ 156.0, 152.7, 151.9 (2 C), 142.0, 141.1, 132.4, 132.3 (2 C), 128.7 (2 C), 126.6, 126.2, 112.8, 107.1, 61.6, 60.9, 56.1, 23.3; ESI-MS: $m/z=460.9$ $[\text{M}+\text{H}]^+$.

3-(2,3,4-Trimethoxyphenyl)-6-(4-methylphenyl)-7H-[1,2,4]triazolo[3,4-b][1,3,4]thiadiazine (4d). Yellow solid; yield: 79%; M.p.: $89\text{--}92^\circ\text{C}$; $^1\text{H-NMR}$ (400 MHz, CDCl_3): δ 7.71 (d, $J=8.2$ Hz, 2 H), 7.33 (d, $J=8.6$ Hz, 1 H), 7.24 (d, $J=8.2$ Hz, 2 H), 6.78 (d, $J=8.6$ Hz, 1 H), 3.97 (s, 2 H), 3.93 (s, 3 H), 3.87 (s, 3 H), 3.76 (s, 3 H), 2.39 (s, 3 H); $^{13}\text{C-NMR}$ (100 MHz, CDCl_3): δ 155.9, 152.8, 152.7, 151.7, 142.5, 142.0, 141.3, 130.7, 129.7 (2 C), 127.2 (2 C), 126.3, 113.0, 107.0, 61.6, 60.9, 56.1, 23.4, 21.5; ESI-MS: $m/z=397.3$ $[\text{M}+\text{H}]^+$, 419.3 $[\text{M}+\text{Na}]^+$.

3-(2,3,4-Trimethoxyphenyl)-6-(4-(trifluoromethyl)phenyl)-7H-[1,2,4]triazolo[3,4-b][1,3,4]thiadiazine (4e). Yellow solid; yield: 67%; M.p.: $95\text{--}96^\circ\text{C}$; $^1\text{H-NMR}$ (400 MHz, CDCl_3): δ 7.94 (d, $J=8.3$ Hz, 2 H), 7.68 (d, $J=8.3$ Hz, 2 H), 7.30 (d, $J=8.6$ Hz, 1 H), 6.78 (d, $J=8.6$ Hz, 1 H), 4.04 (s, 2 H), 3.92 (s, 3 H), 3.86 (s, 3 H), 3.74 (s, 3 H); $^{13}\text{C-NMR}$ (100 MHz, CDCl_3): δ 156.1, 152.6, 152.0, 151.5, 142.0, 141.1, 137.0, 133.2 (d, $J=29.8$ Hz), 127.7 (2 C), 126.2, 126.0, 124.9, 122.2, 112.8, 107.1, 61.6, 60.9, 56.1, 23.5; ESI-MS: $m/z=451.0$ $[\text{M}+\text{H}]^+$.

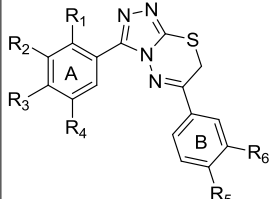
Comp.							IC ₅₀ ^a (μM)		
	R ₁	R ₂	R ₃	R ₄	R ₅	R ₆	SGC-7901	A549	HT-1080
4a	OCH ₃	OCH ₃	OCH ₃	H	F	H	32.6	21.2	31.3
4b	OCH ₃	OCH ₃	OCH ₃	H	Cl	H	24.5	23.2	24.7
4c	OCH ₃	OCH ₃	OCH ₃	H	Br	H	5.55	7.37	3.77
4d	OCH ₃	OCH ₃	OCH ₃	H	CH ₃	H	0.066	0.073	0.028
4e	OCH ₃	OCH ₃	OCH ₃	H	CF ₃	H	2.42	85.4	10.5
4f	OCH ₃	OCH ₃	OCH ₃	H	OCH ₃	H	62.7	50.2	61.4
4g	OCH ₃	OCH ₃	OCH ₃	H	SCH ₃	H	8.02	12.5	2.7
4h	OCH ₃	OCH ₃	OCH ₃	H	OCH ₃	F	43.2	16.3	51.9
4i	OCH ₃	OCH ₃	OCH ₃	H	OCH ₃	NO ₂	13.2	16.5	15.9
4j	OCH ₃	OCH ₃	OCH ₃	H	OCH ₃	NH ₂	1.57	1.58	0.89
4k	OCH ₃	OCH ₃	OCH ₃	H	OCH ₃	OBn	28.9	8.9	28.3
4l	OCH ₃	OCH ₃	OCH ₃	H	OCH ₃	OH	16.3	7.73	0.63
4m	OCH ₃	OCH ₃	OCH ₃	H	F	F	73.2	78.1	81.3
5a	H	OCH ₃	OCH ₃	OCH ₃	Cl	H	1.37	0.27	0.88
5b	H	OCH ₃	OCH ₃	OCH ₃	CH ₃	H	0.027	0.019	0.016
5c	H	OCH ₃	OCH ₃	OCH ₃	CF ₃	H	1.17	7.72	0.75
5d	H	OCH ₃	OCH ₃	OCH ₃	SCH ₃	H	0.13	0.46	0.18
5e	H	OCH ₃	OCH ₃	OCH ₃	OCH ₃	F	4.28	3.21	1.31
5f	H	OCH ₃	OCH ₃	OCH ₃	OCH ₃	NO ₂	11.3	8.88	5.76
5g	H	OCH ₃	OCH ₃	OCH ₃	OCH ₃	NH ₂	1.25	1.08	0.18
5h	H	OCH ₃	OCH ₃	OCH ₃	OCH ₃	OBn	1.66	2.94	1.57
5i	H	OCH ₃	OCH ₃	OCH ₃	OCH ₃	OH	0.026	0.071	0.047
6a	H	OCH ₂ O		H	OCH ₃	F	0.065	0.19	0.13
6b	H	OCH ₂ O		H	OCH ₃	NO ₂	10.5	15.7	0.080
6c	H	OCH ₂ O		H	OCH ₃	NH ₂	0.018	0.026	0.021
6d	H	OCH ₂ O		H	OCH ₃	OBn	8.49	16.3	7.32
6e	H	OCH ₂ O		H	OCH ₃	OH	0.037	0.079	0.035
6f	H	OCH ₃	OCH ₃	H	OCH ₃	NO ₂	5.04	3.68	3.32
6g	H	OCH ₃	OCH ₃	H	OCH ₃	NH ₂	0.023	0.032	0.018
6h	H	OCH ₃	H	H	OCH ₃	NO ₂	2.55	4.2	1.91
6i	H	OCH ₃	H	H	OCH ₃	NH ₂	0.011	0.015	0.014
6j	H	H	OCH ₃	H	OCH ₃	NO ₂	8.04	5.68	2.32
6k	H	H	OCH ₃	H	OCH ₃	NH ₂	0.036	0.038	0.023
CA-4 ^b	—	—	—	—	—	—	0.011	0.009	0.013

Table 1. Antiproliferative activities of the target compounds and CA-4. ^aIC₅₀: 50% inhibitory concentration. Each experiment was carried out in triplicate. ^bpositive control.

3-(2,3,4-Trimethoxyphenyl)-6-(4-methoxyphenyl)-7H-[1,2,4]triazolo[3,4-b][1,3,4]thiadiazine (4f). Yellow solid; yield: 80%; M.p.: 92–95 °C; ¹H-NMR (400 MHz, CDCl₃): δ 7.76 (d, *J* = 8.8 Hz, 2H), 7.29 (d, *J* = 8.6 Hz, 1H), 6.90 (d, *J* = 8.8 Hz, 2H), 6.75 (d, *J* = 8.6 Hz, 1H), 3.95 (s, 2H), 3.90 (s, 3H), 3.84 (s, 3H), 3.81 (s, 3H), 3.74 (s, 3H); ¹³C-NMR (100 MHz, CDCl₃): δ 162.5, 155.9, 152.7, 152.5, 151.6, 142.0, 141.3, 129.0 (2C), 126.2, 125.7, 114.4 (2C), 113.1, 107.0, 61.6, 60.9, 56.1, 55.5, 23.3; ESI-MS: *m/z* = 413.3 [M + H]⁺, 432.3 [M + Na]⁺.

3-(2,3,4-Trimethoxyphenyl)-6-(4-methylthiophenyl)-7H-[1,2,4]triazolo[3,4-b][1,3,4]thiadiazine (4g). Red solid; yield: 75%; M.p.: 86–88 °C; ¹H-NMR (400 MHz, CDCl₃): δ 7.72 (d, *J* = 8.5 Hz, 2H), 7.31 (d, *J* = 8.6 Hz, 1H), 7.23 (d, *J* = 8.5 Hz, 2H), 6.77 (d, *J* = 8.6 Hz, 1H), 3.96 (s, 2H), 3.92 (s, 3H), 3.86 (s, 3H), 3.75 (s, 3H), 2.49 (s, 3H); ¹³C-NMR (100 MHz, CDCl₃): δ 155.9, 152.7, 152.3, 151.7, 144.4, 142.0, 129.5, 127.5 (3C), 126.2, 125.6 (2C), 113.0, 107.0, 61.6, 60.9, 56.1, 23.2, 14.9; ESI-MS: *m/z* = 429.0 [M + H]⁺.

3-(2,3,4-Trimethoxyphenyl)-6-(3-fluoro-4-methoxyphenyl)-7H-[1,2,4]triazolo[3,4-b][1,3,4]thiadiazine (4h). Yellow solid; yield: 71%; M.p.: 92–94 °C; ¹H-NMR (400 MHz, CDCl₃): δ 7.62 (d, *J* = 12.2 Hz,

1 H), 7.54 (d, $J = 8.3$ Hz, 1 H), 7.32 (d, $J = 8.6$ Hz, 1 H), 6.97–7.01 (m, 1 H), 6.79 (d, $J = 8.6$ Hz, 1 H), 3.93 (s, 8 H), 3.88 (s, 3 H), 3.76 (s, 3 H); $^{13}\text{C-NMR}$ (100 MHz, CDCl_3): δ 155.0, 152.6, 151.7, 150.7, 150.3, 150.1, 149.9, 149.8, 141.0, 140.1, 125.2, 123.1 (d, $J = 3.0$ Hz), 113.7 (d, $J = 20.0$ Hz), 111.9, 106.1, 60.6, 59.9, 55.3, 55.1, 22.1; ESI-MS: $m/z = 431.3$ $[\text{M} + \text{H}]^+$, 453.3 $[\text{M} + \text{Na}]^+$.

3-(2,3,4-Trimethoxyphenyl)-6-(3-nitro-4-methoxyphenyl)-7H-[1,2,4]triazolo[3,4-b][1,3,4]thiadiazine (4i). Yellow solid; yield: 79%; M.p.: 134–136 °C; $^1\text{H-NMR}$ (600 MHz, $\text{DMSO-}d_6$): δ 8.39 (d, $J = 2.4$ Hz, 1 H), 8.16 (dd, $J = 8.9$ Hz, $J = 2.4$ Hz, 1 H), 7.52 (d, $J = 8.9$ Hz, 1 H), 7.24 (d, $J = 8.7$ Hz, 1 H), 6.96 (d, $J = 8.7$ Hz, 1 H), 4.45 (s, 2 H), 3.99 (s, 3 H), 3.88 (s, 3 H), 3.79 (s, 3 H), 3.70 (s, 3 H); $^{13}\text{C-NMR}$ (150 MHz, $\text{DMSO-}d_6$): δ 156.0, 154.7, 153.3, 152.5, 151.0, 141.9, 141.6, 139.6, 133.5, 126.4, 125.9, 124.5, 115.9, 112.9, 108.1, 61.8, 60.8, 57.6, 56.4, 23.1; ESI-MS: $m/z = 458.3$ $[\text{M} + \text{H}]^+$, 480.2 $[\text{M} + \text{Na}]^+$.

3-(2,3,4-Trimethoxyphenyl)-6-(3-amino-4-methoxyphenyl)-7H-[1,2,4]triazolo[3,4-b][1,3,4]thiadiazine (4j). Yellow solid; yield: 74%; M.p.: 93–94 °C; $^1\text{H-NMR}$ (400 MHz, CDCl_3): δ 7.30 (d, $J = 8.7$ Hz, 1 H), 7.22 (d, $J = 2.0$ Hz, 1 H), 7.14 (dd, $J = 8.7$ Hz, $J = 2.0$ Hz, 1 H), 6.76 (d, $J = 8.6$ Hz, 2 H), 3.91 (s, 5 H), 3.87 (s, 3 H), 3.85 (s, 3 H), 3.76 (s, 3 H); $^{13}\text{C-NMR}$ (100 MHz, CDCl_3): δ 155.8, 153.0, 152.7, 151.6, 150.3, 142.0, 136.9, 129.8, 126.2, 126.0, 118.5, 113.3, 112.6, 109.8, 107.0, 61.6, 60.9, 56.1, 55.7, 23.3; ESI-MS: $m/z = 428.3$ $[\text{M} + \text{H}]^+$, 450.3 $[\text{M} + \text{Na}]^+$.

3-(2,3,4-Trimethoxyphenyl)-6-(3-benzyloxy-4-methoxyphenyl)-7H-[1,2,4]triazolo[3,4-b][1,3,4]thiadiazine (4k). Gray solid; yield: 82%; M.p.: 85–86 °C; $^1\text{H-NMR}$ (400 MHz, CDCl_3): δ 7.45 (d, $J = 1.8$ Hz, 1 H), 7.32–7.36 (m, 4 H), 7.26–7.28 (m, 3 H), 6.90 (d, $J = 8.6$ Hz, 1 H), 6.80 (d, $J = 8.6$ Hz, 1 H), 5.10 (s, 2 H), 3.93 (s, 6 H), 3.89 (s, 2 H), 3.86 (s, 3 H), 3.71 (s, 3 H); $^{13}\text{C-NMR}$ (100 MHz, CDCl_3): δ 154.9, 152.0, 151.7, 151.2, 150.6, 147.3, 141.0, 140.3, 135.3, 127.6 (2 C), 127.1, 126.4 (2 C), 125.2, 124.9, 120.5, 112.2, 111.2, 110.0, 105.9, 70.1, 60.5, 59.8, 55.1 (2 C), 22.2; ESI-MS: $m/z = 519.2$ $[\text{M} + \text{H}]^+$, 541.1 $[\text{M} + \text{Na}]^+$.

3-(2,3,4-Trimethoxyphenyl)-6-(3-hydroxy-4-methoxyphenyl)-7H-[1,2,4]triazolo[3,4-b][1,3,4]thiadiazine (4l). Brown solid; yield: 83%; M.p.: 88–89 °C; $^1\text{H-NMR}$ (400 MHz, $\text{DMSO-}d_6$): δ 9.48 (s, 1 H), 7.39 (dd, $J = 8.6$ Hz, $J = 2.3$ Hz, 1 H), 7.33 (d, $J = 2.3$ Hz, 1 H), 7.21 (d, $J = 8.6$ Hz, 1 H), 7.03 (d, $J = 8.6$ Hz, 1 H), 6.96 (d, $J = 8.6$ Hz, 1 H), 4.35 (s, 2 H), 3.88 (s, 3 H), 3.82 (s, 3 H), 3.78 (s, 3 H), 3.72 (s, 3 H); $^{13}\text{C-NMR}$ (100 MHz, $\text{DMSO-}d_6$): δ 155.9, 155.0, 152.6, 151.7, 151.0, 147.2, 142.0, 142.0, 126.5, 126.0, 120.7, 113.6, 113.3, 112.1, 108.0, 61.9, 60.9, 56.5, 56.1, 23.1; ESI-MS: $m/z = 429.1$ $[\text{M} + \text{H}]^+$, 451.1 $[\text{M} + \text{Na}]^+$.

3-(2,3,4-Trimethoxyphenyl)-6-(3,4-difluorophenyl)-7H-[1,2,4]triazolo[3,4-b][1,3,4]thiadiazine (4m). Pale-yellow solid; yield: 66%; M.p.: 95–97 °C; $^1\text{H-NMR}$ (400 MHz, CDCl_3): δ 7.68–7.72 (m, 1 H), 7.54–7.56 (m, 1 H), 7.31 (d, $J = 8.6$ Hz, 1 H), 7.22–7.26 (m, 1 H), 6.79 (d, $J = 8.6$ Hz, 1 H), 3.96 (s, 2 H), 3.94 (s, 3 H), 3.89 (s, 3 H), 3.76 (s, 3 H); $^{13}\text{C-NMR}$ (100 MHz, CDCl_3): δ 156.0, 152.6, 151.8, 150.5, 142.0, 130.6, 126.1 (2 C), 123.8, 117.9, 117.8, 116.5, 116.4, 112.8, 107.1, 61.5, 60.8, 56.0, 23.2; ESI-MS: $m/z = 419.3$ $[\text{M} + \text{H}]^+$, 441.2 $[\text{M} + \text{Na}]^+$.

3-(3,4,5-Trimethoxyphenyl)-6-(4-chlorophenyl)-7H-[1,2,4]triazolo[3,4-b][1,3,4]thiadiazine (5a). Pale-yellow solid; yield: 62%; M.p.: 125–127 °C; $^1\text{H-NMR}$ (400 MHz, CDCl_3): δ 7.88 (d, $J = 8.6$ Hz, 2 H), 7.49 (d, $J = 8.6$ Hz, 2 H), 7.42 (s, 2 H), 4.01 (s, 2 H), 3.91 (s, 3 H), 3.88 (s, 6 H); $^{13}\text{C-NMR}$ (100 MHz, CDCl_3): δ 153.2 (2 C), 152.5, 152.1, 141.4, 139.9, 138.5, 131.9, 129.5 (2 C), 128.3 (2 C), 121.1, 105.4 (2 C), 60.9, 56.2 (2 C), 22.9; ESI-MS: $m/z = 417.3$ $[\text{M} + \text{H}]^+$.

3-(3,4,5-Trimethoxyphenyl)-6-(4-methylphenyl)-7H-[1,2,4]triazolo[3,4-b][1,3,4]thiadiazine (5b). Brown solid; yield: 70%; M.p.: 183–185 °C; $^1\text{H-NMR}$ (600 MHz, $\text{DMSO-}d_6$): δ 7.96 (d, $J = 8.0$ Hz, 2 H), 7.41 (s, 2 H), 7.39 (d, $J = 8.0$ Hz, 2 H), 4.42 (s, 2 H), 3.84 (s, 6 H), 3.75 (s, 3 H), 2.39 (s, 3 H); $^{13}\text{C-NMR}$ (150 MHz, $\text{DMSO-}d_6$): δ 156.0, 153.3 (2 C), 151.4, 142.7, 142.7, 139.5, 130.9, 130.1 (2 C), 127.7 (2 C), 121.7, 105.6 (2 C), 60.6, 56.3 (2 C), 22.8, 21.4; ESI-MS: $m/z = 397.3$ $[\text{M} + \text{H}]^+$, 419.3 $[\text{M} + \text{Na}]^+$.

3-(3,4,5-Trimethoxyphenyl)-6-(4-(trifluoromethyl)phenyl)-7H-[1,2,4]triazolo[3,4-b][1,3,4]thiadiazine (5c). Yellow solid; yield: 77%; M.p.: 105–106 °C; $^1\text{H-NMR}$ (400 MHz, CDCl_3): δ 8.06 (d, $J = 8.2$ Hz, 2 H), 7.76 (d, $J = 8.2$ Hz, 2 H), 7.37 (s, 2 H), 4.09 (s, 2 H), 3.89 (s, 3 H), 3.85 (s, 6 H); $^{13}\text{C-NMR}$ (100 MHz, CDCl_3): δ 153.2 (2 C), 152.5, 152.3, 141.6, 140.0, 136.9, 133.6 (d, $J = 32.6$ Hz), 127.6 (2 C), 126.2 (2 C), 124.4, 122.6, 120.9, 105.5 (2 C), 61.0, 56.2 (2 C), 23.1; ESI-MS: $m/z = 451.1$ $[\text{M} + \text{H}]^+$, 473.1 $[\text{M} + \text{Na}]^+$.

3-(3,4,5-Trimethoxyphenyl)-6-(4-methylthiophenyl)-7H-[1,2,4]triazolo[3,4-b][1,3,4]thiadiazine (5d). Gray solid; yield: 79%; M.p.: 92–94 °C; $^1\text{H-NMR}$ (400 MHz, CDCl_3): δ 7.84 (d, $J = 8.6$ Hz, 2 H), 7.45 (s, 2 H), 7.30 (d, $J = 8.6$ Hz, 2 H), 3.99 (s, 2 H), 3.90 (s, 3 H), 3.88 (s, 6 H), 2.53 (s, 3 H); $^{13}\text{C-NMR}$ (150 MHz, CDCl_3): δ 153.1 (2 C), 153.1, 145.0, 139.8, 129.4, 127.2 (3 C), 125.6 (4 C), 105.4 (2 C), 60.9, 56.2 (2 C), 22.8, 14.8; ESI-MS: $m/z = 429.1$ $[\text{M} + \text{H}]^+$, 451.1 $[\text{M} + \text{Na}]^+$.

3-(3,4,5-Trimethoxyphenyl)-6-(3-fluoro-4-methoxyphenyl)-7H-[1,2,4]triazolo[3,4-b][1,3,4]thiadiazine (5e). Pale-yellow solid; yield: 74%; M.p.: 115–118 °C; $^1\text{H-NMR}$ (400 MHz, $\text{DMSO-}d_6$): δ 7.87–7.93 (m, 2 H), 7.39 (s, 3 H), 4.40 (s, 2 H), 3.94 (s, 3 H), 3.85 (s, 6 H), 3.75 (s, 3 H); $^{13}\text{C-NMR}$ (100 MHz, $\text{DMSO-}d_6$): δ 155.0, 153.4 (2 C), 151.4, 150.8, 139.6, 126.3, 125.4, 121.7, 115.1, 114.9, 114.5, 105.7 (2 C), 60.7, 56.9, 56.4 (2 C), 22.8; ESI-MS: $m/z = 431.1$ $[\text{M} + \text{H}]^+$, 453.1 $[\text{M} + \text{Na}]^+$.

3-(3,4,5-Trimethoxyphenyl)-6-(3-nitro-4-methoxyphenyl)-7H-[1,2,4]triazolo[3,4-b][1,3,4]thiadiazine (5f). Maroon solid; yield: 68%; M.p.: 212–213 °C; ¹H-NMR (600 MHz, DMSO-*d*₆): δ 8.56 (s, 1H), 8.31 (d, *J* = 8.0 Hz, 1H), 7.59 (d, *J* = 8.0 Hz, 1H), 7.38 (s, 2H), 4.44 (s, 2H), 4.03 (s, 3H), 3.85 (s, 6H), 3.75 (s, 3H); ¹³C-NMR (150 MHz, DMSO-*d*₆): δ 154.8, 154.3, 153.3 (2C), 151.4, 142.6, 139.8, 139.6, 133.7, 125.9, 124.4, 121.5, 115.5, 105.6 (2C), 60.6, 57.7, 56.3 (2C), 22.8; ESI-MS: *m/z* = 458.3 [M + H]⁺, 480.2 [M + Na]⁺.

3-(3,4,5-Trimethoxyphenyl)-6-(3-amino-4-methoxyphenyl)-7H-[1,2,4]triazolo[3,4-b][1,3,4]thiadiazine (5g). Yellow solid; yield: 65%; M.p.: 112–115 °C; ¹H-NMR (400 MHz, DMSO-*d*₆): δ 7.40–7.41 (m, 3H), 7.26 (dd, *J* = 8.4 Hz, *J* = 2.2 Hz, 1H), 6.95 (d, *J* = 8.4 Hz, 1H), 5.03 (s, 2H), 4.33 (s, 2H), 3.85 (s, 3H), 3.84 (s, 6H), 3.75 (s, 3H); ¹³C-NMR (100 MHz, DMSO-*d*₆): δ 156.2, 153.3 (2C), 151.3, 150.3, 143.0, 139.4, 138.8, 125.9, 121.8, 117.8, 111.0, 110.4, 105.5 (2C), 60.6, 56.3 (2C), 56.0, 22.7; ESI-MS: *m/z* = 428.3 [M + H]⁺, 450.3 [M + Na]⁺.

3-(3,4,5-Trimethoxyphenyl)-6-(3-benzyloxy-4-methoxyphenyl)-7H-[1,2,4]triazolo[3,4-b][1,3,4]thiadiazine (5h). Brown solid; yield: 64%; M.p.: 93–94 °C; ¹H-NMR (400 MHz, CDCl₃): δ 7.58 (s, 1H), 7.48 (d, *J* = 8.0 Hz, 1H), 7.39–7.43 (m, 4H), 7.30–7.33 (m, 3H), 6.97 (d, *J* = 8.2 Hz, 1H), 5.14 (s, 2H), 3.96 (s, 3H), 3.91–3.93 (m, 5H), 3.87 (s, 6H); ¹³C-NMR (100 MHz, CDCl₃): δ 153.5, 153.2(3C), 148.7, 139.9, 136.2, 128.7 (2C), 128.3 (2C), 127.5 (2C), 125.9, 121.8 (2C), 121.5, 112.5, 111.3, 105.7 (2C), 71.6, 61.0, 56.4 (2C), 56.2, 23.0; ESI-MS: *m/z* = 519.2 [M + H]⁺, 541.1 [M + Na]⁺.

3-(3,4,5-Trimethoxyphenyl)-6-(3-hydroxy-4-methoxyphenyl)-7H-[1,2,4]triazolo[3,4-b][1,3,4]thiadiazine (5i). Yellow solid; yield: 60%; M.p.: 95–97 °C; ¹H-NMR (400 MHz, DMSO-*d*₆): δ 9.53 (s, 1H), 7.56 (d, *J* = 2.2 Hz, 1H), 7.50 (dd, *J* = 8.5 Hz, *J* = 2.2 Hz, 1H), 7.38 (s, 2H), 7.09 (d, *J* = 8.5 Hz, 1H), 4.36 (s, 2H), 3.86 (s, 3H), 3.85 (s, 6H), 3.76 (s, 3H); ¹³C-NMR (100 MHz, DMSO-*d*₆): δ 155.8, 153.4, 151.9, 151.5, 147.5, 143.0, 139.5, 126.0, 121.8, 120.8, 113.6, 112.1, 105.6, 60.7, 56.4 (2C), 56.2, 22.7; ESI-MS: *m/z* = 429.1 [M + H]⁺, 451.1 [M + Na]⁺.

3-(3,4-Methylenedioxyphenyl)-6-(3-fluoro-4-methoxyphenyl)-7H-[1,2,4]triazolo[3,4-b][1,3,4]thiadiazine (6a). Pale-yellow solid; yield: 76%; M.p.: 93–95 °C; ¹H-NMR (400 MHz, DMSO-*d*₆): δ 7.85 (s, 1H), 7.83 (s, 1H), 7.54 (dd, *J* = 8.2 Hz, *J* = 1.6 Hz, 1H), 7.50 (d, *J* = 1.6 Hz, 1H), 7.35–7.39 (m, 1H), 7.12 (d, *J* = 8.2 Hz, 1H), 6.13 (s, 2H), 4.37 (s, 2H), 3.94 (s, 3H); ¹³C-NMR (100 MHz, DMSO-*d*₆): δ 155.1, 151.7, 150.7, 149.4, 148.0, 142.6, 126.3, 125.5, 123.1, 120.1, 115.3, 115.1, 114.5, 109.1, 108.2, 102.2, 56.8, 22.9; ESI-MS: *m/z* = 385.1 [M + H]⁺, 407.1 [M + Na]⁺.

3-(3,4-Methylenedioxyphenyl)-6-(3-nitro-4-methoxyphenyl)-7H-[1,2,4]triazolo[3,4-b][1,3,4]thiadiazine (6b). Pale-yellow solid; yield: 80%; M.p.: 90–92 °C; ¹H-NMR (600 MHz, DMSO-*d*₆): δ 8.49 (s, 1H), 8.27 (d, *J* = 7.6 Hz, 1H), 7.58 (d, *J* = 7.6 Hz, 1H), 7.54 (d, *J* = 7.2 Hz, 1H), 7.50 (s, 1H), 7.11 (d, *J* = 7.2 Hz, 1H), 6.13 (s, 2H), 4.42 (s, 2H), 4.03 (s, 3H); ¹³C-NMR (150 MHz, DMSO-*d*₆): δ 154.8, 154.3, 151.7, 149.4, 147.9, 142.5, 139.7, 133.5, 126.0, 124.8, 123.1, 119.9, 115.6, 109.0, 108.2, 102.1, 57.7, 22.9; ESI-MS: *m/z* = 412.1 [M + H]⁺, 434.1 [M + Na]⁺.

3-(3,4-Methylenedioxyphenyl)-6-(3-amino-4-methoxyphenyl)-7H-[1,2,4]triazolo[3,4-b][1,3,4]thiadiazine (6c). Yellow solid; yield: 78%; M.p.: 88–90 °C; ¹H-NMR (400 MHz, DMSO-*d*₆): δ 7.58 (dd, *J* = 8.2 Hz, *J* = 1.4 Hz, 1H), 7.49 (d, *J* = 1.4 Hz, 1H), 7.28 (d, *J* = 2.1 Hz, 1H), 7.22 (dd, *J* = 8.4 Hz, *J* = 2.1 Hz, 1H), 7.12 (d, *J* = 8.2 Hz, 1H), 6.95 (d, *J* = 8.4 Hz, 1H), 6.13 (s, 2H), 5.06 (s, 2H), 4.30 (s, 2H), 3.85 (s, 3H); ¹³C-NMR (100 MHz, DMSO-*d*₆): δ 156.4, 151.5, 150.2, 149.2, 147.9, 142.9, 138.6, 126.1, 122.9, 120.3, 117.7, 111.4, 110.5, 109.0, 108.1, 102.0, 56.0, 23.0; ESI-MS: *m/z* = 382.0 [M + H]⁺.

3-(3,4-Methylenedioxyphenyl)-6-(3-benzyloxy-4-methoxyphenyl)-7H-[1,2,4]triazolo[3,4-b][1,3,4]thiadiazine (6d). Pale-yellow solid; yield: 81%; M.p.: 86–88 °C; ¹H-NMR (400 MHz, CDCl₃): δ 7.64–7.65 (m, 2H), 7.59 (d, *J* = 1.6 Hz, 1H), 7.39–7.45 (m, 3H), 7.30–7.37 (m, 3H), 6.96 (d, *J* = 8.4 Hz, 1H), 6.88 (d, *J* = 8.4 Hz, 1H), 6.02 (s, 2H), 5.19 (s, 2H), 3.96 (s, 3H), 3.90 (s, 2H); ¹³C-NMR (100 MHz, CDCl₃): δ 153.3, 153.1, 149.3, 148.6, 147.8, 136.4, 128.7 (3C), 128.2, 127.5 (2C), 127.4, 125.8, 123.0, 121.7, 120.1, 111.8, 111.1, 108.5 (2C), 101.5, 71.1, 56.2, 22.9; ESI-MS: *m/z* = 473.0 [M + H]⁺, 945.1 [2M + H]⁺.

3-(3,4-Methylenedioxyphenyl)-6-(3-hydroxy-4-methoxyphenyl)-7H-[1,2,4]triazolo[3,4-b][1,3,4]thiadiazine (6e). Yellow solid; yield: 68%; M.p.: 85–87 °C; ¹H-NMR (400 MHz, DMSO-*d*₆): δ 9.55 (s, 1H), 7.56 (dd, *J* = 8.2 Hz, *J* = 1.6 Hz, 1H), 7.50 (d, *J* = 1.6 Hz, 1H), 7.45–7.47 (m, 2H), 7.08–7.13 (m, 2H), 6.14 (s, 2H), 4.33 (s, 2H), 3.86 (s, 3H); ¹³C-NMR (100 MHz, DMSO-*d*₆): δ 156.0, 151.8, 151.6, 149.3, 148.0, 147.3, 142.9, 126.1, 123.0, 120.8, 120.3, 113.9, 112.2, 109.1, 108.2, 102.1, 56.2, 22.9; ESI-MS: *m/z* = 383.1 [M + H]⁺, 405.1 [M + Na]⁺.

3-(3,4-Dimethoxyphenyl)-6-(3-nitro-4-methoxyphenyl)-7H-[1,2,4]triazolo[3,4-b][1,3,4]thiadiazine (6f). Yellow solid; yield: 78%; M.p.: 190–192 °C; ¹H-NMR (600 MHz, DMSO-*d*₆): δ 8.53 (d, *J* = 2.3 Hz, 1H), 8.30 (dd, *J* = 8.9 Hz, *J* = 2.3 Hz, 1H), 7.64 (d, *J* = 1.8 Hz, 1H), 7.60 (dd, *J* = 8.4 Hz, *J* = 1.8 Hz, 1H), 7.58 (d, *J* = 8.9 Hz, 1H), 7.14 (d, *J* = 8.4 Hz, 1H), 4.43 (s, 2H), 4.03 (s, 3H), 3.84 (s, 3H), 3.83 (s, 3H); ¹³C-NMR (150 MHz, DMSO-*d*₆): δ 154.7, 154.1, 151.7, 150.9, 148.9, 142.2, 139.8, 133.6, 126.0, 124.5, 121.4, 118.7, 115.5, 112.0, 111.3, 56.0, 55.9, 55.3, 22.8; ESI-MS: *m/z* = 428.1 [M + H]⁺, 450.1 [M + Na]⁺.

3-(3,4-Dimethoxyphenyl)-6-(3-amino-4-methoxyphenyl)-7H-[1,2,4]triazolo[3,4-b][1,3,4]thiadiazine (6g). Pale-yellow solid; yield: 68%; M.p.: 213–215 °C; ¹H-NMR (600 MHz, DMSO-*d*₆): δ 7.66 (d, *J* = 8.9 Hz, 1 H), 7.65 (s, 1 H), 7.36 (s, 1 H), 7.24 (dd, *J* = 8.5 Hz, *J* = 1.6 Hz, 1 H), 7.16 (d, *J* = 8.9 Hz, 1 H), 6.95 (d, *J* = 8.5 Hz, 1 H), 5.07 (s, 2 H), 4.32 (s, 2 H), 3.86 (s, 3 H), 3.84 (s, 3 H), 3.83 (s, 3 H); ¹³C-NMR (150 MHz, DMSO-*d*₆): δ 156.2, 151.5, 150.7, 150.2, 148.9, 142.6, 138.7, 126.1, 121.2, 119.0, 117.7, 112.1, 111.2 (2 C), 110.4, 55.9, 55.8, 55.3, 22.8; ESI-MS: *m/z* = 398.4 [M + H]⁺, 420.3 [M + Na]⁺.

3-(3-Methoxyphenyl)-6-(3-nitro-4-methoxyphenyl)-7H-[1,2,4]triazolo[3,4-b][1,3,4]thiadiazine (6h). White solid; yield: 83%; M.p.: 207–208 °C; ¹H-NMR (600 MHz, DMSO-*d*₆): δ 8.51 (d, *J* = 2.1 Hz, 1 H), 8.28 (dd, *J* = 8.9 Hz, *J* = 2.1 Hz, 1 H), 7.57–7.60 (m, 3 H), 7.46–7.49 (m, 1 H), 7.12 (dd, *J* = 8.4 Hz, *J* = 2.1 Hz, 1 H), 4.45 (s, 2 H), 4.03 (s, 3 H), 3.83 (s, 3 H); ¹³C-NMR (150 MHz, DMSO-*d*₆): δ 159.6, 154.8, 154.4, 151.7, 142.9, 139.7, 133.6, 130.3, 127.4, 125.9, 124.7, 120.6, 116.7, 115.6, 113.2, 57.7, 55.6, 22.9; ESI-MS: *m/z* = 398.1 [M + H]⁺.

3-(3-Methoxyphenyl)-6-(3-amino-4-methoxyphenyl)-7H-[1,2,4]triazolo[3,4-b][1,3,4]thiadiazine (6i). Red-brown solid; yield: 65%; M.p.: 138–140 °C; ¹H-NMR (600 MHz, DMSO-*d*₆): δ 7.64 (d, *J* = 7.8 Hz, 1 H), 7.60 (s, 1 H), 7.48–7.51 (m, 1 H), 7.34 (d, *J* = 2.2 Hz, 1 H), 7.24 (dd, *J* = 8.4 Hz, *J* = 2.2 Hz, 1 H), 7.12 (dd, *J* = 8.2 Hz, *J* = 2.1 Hz, 1 H), 6.95 (d, *J* = 8.4 Hz, 1 H), 5.07 (s, 2 H), 4.34 (s, 2 H), 3.86 (s, 3 H), 3.83 (s, 3 H); ¹³C-NMR (150 MHz, DMSO-*d*₆): δ 159.6, 156.5, 151.5, 150.2, 143.3, 138.7, 130.3, 127.7, 126.0, 120.5, 117.8, 116.5, 113.1, 111.3, 110.4, 55.9, 55.6, 22.9; ESI-MS: *m/z* = 368.1 [M + H]⁺.

3-(4-Methoxyphenyl)-6-(3-nitro-4-methoxyphenyl)-7H-[1,2,4]triazolo[3,4-b][1,3,4]thiadiazine (6j). Yellow solid; yield: 85%; M.p.: 97–99 °C; ¹H-NMR (600 MHz, DMSO-*d*₆): δ 8.50 (s, 1 H), 8.28 (d, *J* = 8.9 Hz, 1 H), 7.95 (d, *J* = 8.4 Hz, 2 H), 7.56 (d, *J* = 8.9 Hz, 1 H), 7.12 (d, *J* = 8.4 Hz, 2 H), 4.43 (s, 2 H), 4.03 (s, 3 H), 3.84 (s, 3 H); ¹³C-NMR (150 MHz, DMSO-*d*₆): δ 161.1, 154.7, 154.2, 151.8, 142.2, 139.7, 133.5, 129.9 (2 C), 126.0, 124.7, 118.6, 115.5, 114.6 (2 C), 57.6, 55.7, 22.9; ESI-MS: *m/z* = 398.1 [M + H]⁺, 420.1 [M + Na]⁺.

3-(4-Methoxyphenyl)-6-(3-amino-4-methoxyphenyl)-7H-[1,2,4]triazolo[3,4-b][1,3,4]thiadiazine (6k). Pale-yellow solid; yield: 71%; M.p.: 214–215 °C; ¹H-NMR (600 MHz, DMSO-*d*₆): δ 8.00 (d, *J* = 8.9 Hz, 2 H), 7.32 (d, *J* = 2.3 Hz, 1 H), 7.23 (dd, *J* = 8.5 Hz, *J* = 2.3 Hz, 1 H), 7.14 (d, *J* = 8.9 Hz, 2 H), 6.95 (d, *J* = 8.5 Hz, 1 H), 5.09 (s, 2 H), 4.32 (s, 2 H), 3.86 (s, 3 H), 3.85 (s, 3 H); ¹³C-NMR (150 MHz, DMSO-*d*₆): δ 161.0, 156.3, 151.6, 150.2, 142.5, 138.7, 129.7 (2 C), 126.1, 119.0, 117.8, 114.6 (2 C), 111.3, 110.4, 55.9, 55.7, 22.9; ESI-MS: *m/z* = 368.3 [M + H]⁺, 390.3 [M + Na]⁺.

MTT assay. The antiproliferative activities of all of the target compounds and CA-4 were determined by a standard MTT assay following a previously reported method³³. The SGC-7901, A549 and HT-1080 cell lines were purchased from the American Type Culture Collection (ATCC, Manassas, VA, USA). The *in vitro* antiproliferative activities of CA-4 and all of the target compounds were determined by a MTT (Sigma) assay. Briefly, approximately 3 × 10⁴ cells were seeded in a 96-well plate. After 24 h of incubation at 37 °C, cells were exposed to compounds of differing concentrations for 24 h. After treatment, cells were washed with 1X PBS followed by addition of 100 μL of 0.05% MTT reagent to each well, followed by incubation for 4 h at 37 °C. After incubation, the supernatant from each well was carefully removed and the formazan crystals were dissolved in 100 μL of DMSO. The colour density was measured spectrophotometrically at 490 nm using a microplate reader (SpectraMax Plus384, Molecular Devices Corp., USA). The data were calculated and plotted as percent viability compared to control.

Tubulin polymerization assay. Tubulin polymerization assay³³ was conducted with reagents as described in the kit manufacturer (Cytoskeleton, Cat.#BK011P) in a 96-well plate. In brief, tubulin was re-suspended in ice-cold G-PEM buffer (80 mM PIPES, 2 mM MgCl₂, 0.5 mM EGTA, 1 mM GTP, 20% (v/v) glycerol) and added to wells on a 96-well plate containing the designated concentration of drugs or vehicle. Samples were mixed well, and tubulin assembly was monitored (emission wavelength: 450 ± 20 nm; excitation wavelength: 360 ± 20 nm) at 1 min intervals for 90 min at 37 °C in a SpectraMax 340PC spectrophotometer (Biotek Synergy HT, Winooski, VT, USA). IC₅₀ values were calculated from data at the 20 min time point using GraphPad Prism software. Experiments were repeated three times.

Immunofluorescence assay. Immunostaining assay³⁵ was carried out to detect microtubule associated tubulin protein after exposure to **6i** and CA-4. The SGC-7901 cells were seeded at a density of 1 × 10⁴ per well on a 24-well plate and grown for 24 h. Cells were treated with CA-4 or **6i** for 12 h. Cells in the control group were treated with culture medium. The control and treated cells were fixed with 4% formaldehyde in PBS for 30 min at -20 °C, then washed twice with PBS and permeabilized with 0.1% (v/v) Triton X-100 in PBS for 5 min. Then, the cells were blocked with 3% bovine serum albumin (BSA) in PBS for 30 min. The primary α-tubulin antibody was diluted (1:100) with 2% BSA in PBS and incubated overnight at 4 °C. The cells were washed with PBS to remove unbound primary antibody and then cells were incubated with FITC-conjugated antimouse secondary antibody, diluted (1:100) with 2% BSA in PBS, for 2 h at 37 °C. The cells were washed with PBS to remove unbound secondary antibody, nucleus was stained with 4,6-diamino-2-phenylindol dihydrochloride (DAPI) and then, immunofluorescence was detected using a fluorescence microscope (Olympus, Tokyo, Japan).

Cell cycle analysis. Cell cycle analysis studies were performed by following a previously reported method³⁵. SGC-7901 cells (8 × 10⁴ cells) were incubated with various concentrations of CA-4, **6i** or 0.05% DMSO for the indicated times. The cells were collected by centrifugation, washed with PBS and fixed in ice-cold 70% ethanol.

The fixed cells were harvested by centrifugation and resuspended in 500 μl of PBS containing 1 mg/mL RNase. After 30 min of incubation at 37°C, the cells were stained with 50 mg/mL propidium iodide (PI) at 4°C in the dark for 30 min. The samples were then analyzed by FACScan flow cytometry (Becton-Dickinson, Franklin Lakes, NJ, USA). The experiments were repeated at least three times.

Competitive tubulin-binding assay. For the colchicine competitive binding assay, tubulin was co-incubated with indicated concentrations of MPSP-001 and paclitaxel at 37°C for 1 h. Then colchicine was added to a final concentration of 5 $\mu\text{mol L}^{-1}$. Fluorescence was determined using a Hitachi F-2500 spectrofluorometer (Tokyo, Japan) at the excitation wavelength of 365 nm and the emission wavelength of 435 nm. Blank values (buffer alone) as the background were subtracted from all samples. Then the inhibition rate (IR) was calculated as follows: $\text{IR} = F/F_0$ where F_0 is the fluorescence of 5 $\mu\text{mol L}^{-1}$ colchicine-tubulin complex, and F is the fluorescence of a given concentration of CA-4 or **6i** or taxol (1.6 $\mu\text{mol L}^{-1}$, 5 $\mu\text{mol L}^{-1}$, 15 $\mu\text{mol L}^{-1}$) in competition with 5 $\mu\text{mol L}^{-1}$ colchicine-tubulin complex. Paclitaxel, not binding in the colchicine site of tubulin, was added as a negative control. The experiments were repeated at least three times.

Molecular docking studies. Molecular docking studies were performed by following a previously reported method³³. The molecular modeling studies were performed using Accelrys Discovery Studio 3.0. The crystal structure of tubulin complexed with DAMA-colchicine (PDB: 1SA0) was retrieved from the RCSB Protein Data Bank (<http://www.rcsb.org/pdb>). In the docking process, the protein protocol was prepared via several operations, including the standardization of atom names, insertion of missing atoms in residues and removal of alternate conformations, insertion of missing loop regions based on SEQRES data, optimization of short and medium sized loop regions with the Looper Algorithm, minimization of remaining loop regions, calculation of pK, and protonation of the structure. The receptor model was then typed with the CHARMM force field, and a binding sphere with a radius of 9.0 Å was defined with the original ligand (DAMA-colchicine) as the binding site. The **6i**, CA-4 and vinylogous CA-4 were drawn with Chemdraw and fully minimized using the CHARMM force field. Finally, **6i**, CA-4 and vinylogous CA-4 were docked into the binding site using the CDocker protocol with the default settings.

References

- Brouhard, G. J. & Rice, L. M. The contribution of $\alpha\beta$ -tubulin curvature to microtubule dynamics. *J. Cell Biol.* **207**, 323–334 (2014).
- Kueh, H. Y. & Mitchison, T. J. Structural plasticity in actin and tubulin polymer dynamics. *Science*. **325**, 960–963 (2009).
- Vindya, N. G., Sharma, N., Yadav, M. & Ethiraj, K. R. Tubulins—the target for anticancer therapy. *Curr. Top. Med. Chem.* **15**, 73–82 (2015).
- Liu, Y. M., Chen, H. L., Lee, H. Y. & Liou, J. P. Tubulin inhibitors: a patent review. *Expert Opin. Ther. Pat.* **24**, 69–88 (2014).
- Zhou, J. & Giannakakou, P. Targeting microtubules for cancer chemotherapy. *Curr. Med. Chem. Anticancer Agents*. **5**, 65–71 (2005).
- van Vuuren, R. J., Visagie, M. H., Theron, A. E. & Joubert, A. M. Antimitotic drugs in the treatment of cancer. *Cancer Chemother Pharmacol.* **76**, 1101–1112 (2015).
- Jordan, A., Hadfield, J. A., Lawrence, N. J. & McGown, A. T. Tubulin as a target for anticancer drugs: agents which interact with the mitotic spindle. *Med. Res. Rev.* **18**, 259–296 (1998).
- Yue, Q. X., Liu, X. & Guo, D. A. Microtubule-binding natural products for cancer therapy. *Planta Med.* **76**, 1037–1043 (2010).
- Lu, Y., Chen, J., Xiao, M., Li, W. & Miller, D. D. An overview of tubulin inhibitors that interact with the colchicine binding site. *Pharm Res.* **29**, 2943–2971 (2012).
- Pettit, G. R. *et al.* Isolation and structure of the strong cell growth and tubulin inhibitor combretastatin A-4. *Experientia*. **45**, 209–211 (1989).
- Kaur, R., Kaur, G., Gill, R. K., Soni, R. & Bariwal, J. Recent developments in tubulin polymerization inhibitors: An overview. *Eur. J. Med. Chem.* **87**, 89–124 (2014).
- Patil, P. O. *et al.* Recent advancement in discovery and development of natural product combretastatin-inspired anticancer agents. *Anticancer Agents Med. Chem.* **15**, 955–969 (2015).
- Zhou, P. *et al.* Potent Antitumor Activities and Structure Basis of the Chiral B-Lactam Bridged Analogue of Combretastatin A-4 Binding to Tubulin. *J. Med. Chem.* **59**, 10329–10334 (2016).
- Brown, A. *et al.* Sydnone Cycloaddition Route to Pyrazole-Based Analogs of Combretastatin A4. *J. Med. Chem.* **59**, 9473–9488 (2016).
- Banimustafa, M. *et al.* Synthesis and biological evaluation of 3-(trimethoxyphenyl)-2(3H)-thiazole thiones as combretastatin analogs. *Eur. J. Med. Chem.* **70**, 692–702 (2013).
- EdosA, S. *et al.* Synthesis and evaluation of diaryl sulfides and diaryl selenide compounds for antitubulin and cytotoxic activity. *Bioorganic & Medicinal Chemistry Letters*. **23**, 4669–4673 (2013).
- Yan, J. *et al.* Synthesis, biological evaluation and mechanism study of a class of cyclic combretastatin A-4 analogues as novel antitumor agents. *RSC Adv.* **5**, 98527–98537 (2015).
- Lee, H. *et al.* Antimitotic and antivascular activity of heteroaroyl-2-hydroxy-3,4,5-trimethoxybenzenes. *Bioorg. Med. Chem.* **23**, 4230–4236 (2015).
- Romagnoli, R. *et al.* Synthesis, antimitotic and antivascular activity of 1-(3',4',5'-trimethoxybenzoyl)-3-arylamino-5-amino-1,2,4-triazoles. *J. Med. Chem.* **57**, 6795–6808 (2014).
- Duan, Y.T. *et al.* Design, synthesis and antitumor activity of novel link-bridge and B-ring modified combretastatin A-4 (CA-4) analogues as potent antitubulin agents. *Sci. Rep.* **6** (2016).
- Gerova, M. S. *et al.* Combretastatin A-4 analogues with benzoxazolone scaffold: Synthesis, structure and biological activity. *Eur. J. Med. Chem.* **120**, 121–133 (2016).
- Do, C. V. *et al.* Synthesis and biological evaluation of thiophene and benzo b thiophene analogs of combretastatin A-4 and isocombretastatin A-4: A comparison between the linkage positions of the 3,4,5-trimethoxystyrene unit. *Bioorg. Med. Chem. Lett.* **26**, 174–180 (2016).
- Wu, X. *et al.* Recent Advances in Heterocyclic Tubulin Inhibitors Targeting the Colchicine Binding Site. *Anti-Cancer Agents in Med. Chem.* **16**, 1325–1338 (2016).
- Kamal, A. *et al.* Synthesis and biological evaluation of 1,2,3-triazole linked aminocombretastatin conjugates as mitochondrial mediated apoptosis inducers. *Bioorg. Med. Chem.* **22**, 5155–5167 (2014).
- Zheng, S. *et al.* Design, Synthesis, and Biological Evaluation of Novel PyridineBridged Analogues of Combretastatin-A4 as Anticancer Agents. *J. Med. Chem.* **57**, 3369–3381 (2014).

26. Romagnoli, R. *et al.* Design and synthesis of potent *in vitro* and *in vivo* anticancer agents based on 1-(3',4',5'-trimethoxyphenyl)-2-aryl-1H-imidazole. *Sci. Rep.* **6**, 26602, doi:10.1038/srep26602 (2016).
27. Rajak, H. *et al.* Design of combretastatin A-4 analogs as tubulin targeted vascular disrupting agent with special emphasis on their *cis*-restricted isomers. *Curr. Pharm. Des.* **19**, 1923–1955 (2013).
28. Ohsumi, K. *et al.* Syntheses and antitumor activity of *cis*-restricted combretastatins: 5-membered heterocyclic analogues. *Bioorg. Med. Chem. Lett.* **8**, 3153–3158 (1998).
29. Simoni, D. *et al.* Heterocyclic and phenyl double-bond-locked combretastatin analogues possessing potent apoptosis-inducing activity in HL60 and in MDR cell lines. *J. Med. Chem.* **48**, 723–736 (2005).
30. Kaffy, J., Pontikis, R., Florent, J. C. & Monneret, C. Synthesis and biological evaluation of vinylogous combretastatin A-4 derivatives. *Org. Biomol. Chem.* **3**, 2657–2660 (2005).
31. Kaur, R., Dwivedi, A. R., Kumar, B. & Kumar, V. Recent developments on 1,2,4-triazole nucleus in anticancer compounds: A Review. *Anticancer Agents Med. Chem.* **16**, 465–489 (2016).
32. Kharb, R., Sharma, P. C. & Yar, M. S. Pharmacological significance of triazole scaffold. *J. Enzyme. Inhib. Med. Chem.* **26**, 1–21 (2011).
33. Xu, Q. *et al.* Synthesis and biological evaluation of 3-alkyl-1,5-diaryl-1H-pyrazoles as rigid analogues of combretastatin A-4 with potent antiproliferative activity. *PLoS ONE*. **10**, e0128710, doi:10.1371/journal.pone.0128710 (2015).
34. Wen, Z. *et al.* 3-(3,4,5-Trimethoxyphenylselenyl)-1H-indoles and their selenoxides as combretastatin A-4 analogs: microwave-assisted synthesis and biological evaluation. *Eur. J. Med. Chem.* **27**, 184–194 (2015).
35. Guan, Q. *et al.* Synthesis and biological evaluation of novel 3,4-diaryl-1,2,5-selenadiazol analogues of combretastatin A-4. *Eur. J. Med. Chem.* **87**, 1–9 (2014).
36. Guan, Q. *et al.* Synthesis and evaluation of benzimidazole carbamates bearing indole moieties for antiproliferative and antitubulin activities. *Eur. J. Med. Chem.* **87**, 306–315 (2014).
37. Wen, Z. *et al.* Ultrasound-promoted two-step synthesis of 3-arylselenylindoles and 3-arylthioindoles as novel combretastatin A-4 analogues. *Scientific Reports*. **6**, 23986, doi:10.1038/srep23986 (2016).
38. Negi, A. S. *et al.* Natural antitubulin agents: importance of 3,4,5-trimethoxyphenyl fragment. *Bioorg. Med. Chem.* **23**, 373–389 (2015).
39. Kamal, A. *et al.* Synthesis of phenstatin/isocombretastatin-chalcone conjugates as potent tubulin polymerization inhibitors and mitochondrial apoptotic inducers. *Org. Biomol. Chem.* **13**, 3963–3981 (2015).
40. Zhang, C. *et al.* S9, a novel anticancer agent, exerts its anti-proliferative activity by interfering with both PI3K-Akt-mTOR signaling and microtubule cytoskeleton. *PLoS One*. **4**, e4881, doi:10.1371/journal.pone.0004881 (2009).

Acknowledgements

We gratefully acknowledge the National Natural Science Foundation of China (81673293, 81502932, 81602969), Program for Liaoning Excellent Talents in University (LR2013046) and State Key Laboratory of Natural Medicines and Active Substance (No. GTZK201603) for their generous financial support.

Author Contributions

Q.X., K.B., Y.W., J.X., M.S. and H.T. performed the experiments. Q.X., Q.G., D.Z., K.B., Y.W. and W.Z. analyzed, interpreted the data and wrote the paper.

Additional Information

Supplementary information accompanies this paper at doi:10.1038/s41598-017-10860-7

Competing Interests: The authors declare that they have no competing interests.

Publisher's note: Springer Nature remains neutral with regard to jurisdictional claims in published maps and institutional affiliations.



Open Access This article is licensed under a Creative Commons Attribution 4.0 International License, which permits use, sharing, adaptation, distribution and reproduction in any medium or format, as long as you give appropriate credit to the original author(s) and the source, provide a link to the Creative Commons license, and indicate if changes were made. The images or other third party material in this article are included in the article's Creative Commons license, unless indicated otherwise in a credit line to the material. If material is not included in the article's Creative Commons license and your intended use is not permitted by statutory regulation or exceeds the permitted use, you will need to obtain permission directly from the copyright holder. To view a copy of this license, visit <http://creativecommons.org/licenses/by/4.0/>.

© The Author(s) 2017